

Impact of the reduction process on the long-range antiferromagnetism in $\text{Nd}_{1.85}\text{Ce}_{0.15}\text{CuO}_4$

P. Richard,^{1,2,*} M. Poirier,¹ S. Jandl,¹ and P. Fournier¹

¹*Regroupement Québécois sur les Matériaux de Pointe, Département de Physique, Université de Sherbrooke, Sherbrooke, Canada J1K 2R1*

²*Department of Physics, Boston College, Chestnut Hill, Massachusetts 02467, USA*

(Received 17 June 2005; revised manuscript received 27 September 2005; published 21 November 2005)

We have performed an ultrasonic study of $\text{Nd}_{2-x}\text{Ce}_x\text{CuO}_4$ samples which show frequency-dependent ultrasonic anomalies below 10 K in both the C_{66} elastic moduli and the corresponding attenuation α similar to those observed in the undoped material. While the cerium doping only changes the temperature and magnetic scales over which the anomalies are detected, no anomaly is observed for the reduced and superconducting state of a $\text{Nd}_{1.85}\text{Ce}_{0.15}\text{CuO}_4$ sample. This indicates that the sudden suppression of the Cu^{2+} long-range three-dimensional antiferromagnetic order following the reduction process favors the emergence of the competing superconducting state.

DOI: [10.1103/PhysRevB.72.184514](https://doi.org/10.1103/PhysRevB.72.184514)

PACS number(s): 74.72.Jt, 74.25.Ha, 74.25.Ld

I. INTRODUCTION

In the past few years, much effort has been devoted to the understanding of superconductivity in the 2-1-4 electron-doped superconductors ($R_{2-x}\text{Ce}_x\text{CuO}_4$, $R=\text{Pr, Nd, Sm}$). In addition to the sign of the carriers and the controversial issue of their order parameter, the electron-doped cuprates have raised a particular interest due to their peculiar magnetic properties. In contrast to the hole-doped superconductors, for which the long-range antiferromagnetic (AF) order is suppressed at low doping, the AF order is more robust in the electron-doped materials and persists up to optimal doping. Even though Kang *et al.*¹ proposed that long-range AF order and superconductivity are competing states, another neutron study rather concluded to the coexistence of these two states.² Hence, it is an important issue to determine the effect, on the AF ordering, of the reduction process that triggers superconductivity in these materials by removing a tiny amount of oxygen, which is estimated to be much less than 1% for the optimally doped samples.³⁻⁷ According to neutron measurements,⁸⁻¹⁰ the Néel temperature of the as-grown samples decreases after the reduction process, particularly for $x \geq 0.1$.^{9,10} Unfortunately, literature not only lacks of results relative to the persistence of long-range order in these systems, but also of microscopic interpretations for the role of reduction process on their magnetic properties. Recent Raman and crystal-field infrared transmission studies question this issue. Their interpretation ruled out the generally accepted assumption that oxygens are removed from interstitial sites following reduction and suggested that a particular defect, called β and tentatively attributed to in-plane oxygen vacancies, is created instead at optimal doping.^{11,12}

In comparison to Pr_2CuO_4 and Sm_2CuO_4 for which the rare earth magnetic sublattices are not strongly coupled to the Cu^{2+} one, the strong coupling between the Nd^{3+} and Cu^{2+} moments in Nd_2CuO_4 allows one to investigate the Cu^{2+} AF ordering via the Nd^{3+} magnetic moments. Among several techniques, ultrasonic propagation has proved to be particularly sensitive to the magnetic structure of Nd_2CuO_4 . Although the ultrasonic waves do not seem to be affected by the Néel AF order around 280 K, elastic anomalies have

been observed at 33 (Refs. 13–15) and 67 K,¹⁵ due to the well known spin reorientation transitions of the Nd_2CuO_4 noncollinear long-range order. Moreover, short-range order among the Nd^{3+} lattice gives rise to gigantic elastic anomalies below 10 K, which have been associated to domains in the frustrated magnetic structure of Nd_2CuO_4 resulting from the competition between the $\text{Nd}^{3+}\text{-Cu}^{2+}$ and $\text{Nd}^{3+}\text{-Nd}^{3+}$ interactions.¹⁵ In the Ce^{4+} doped compounds, the spin reorientation anomalies are absent but the low temperature ones, although strongly suppressed, broadened and shifted to higher temperatures, are still observed.¹⁴ These ultrasonic data were obtained on as-grown nonsuperconducting crystals only. Although essential to induce superconductivity, the influence of the reduction process on the low-temperature anomalies has not been investigated so far.

In this paper, we thus investigate the influence of the Ce doping and the reduction process on the low-temperature magnetic properties of $\text{Nd}_{2-x}\text{Ce}_x\text{CuO}_4$ by analyzing the ultrasonic anomalies appearing on the elastic constant C_{66} and on the attenuation. It is found that cerium doping modifies the temperature and magnetic field scales over which the anomalies are observed without changing the overall magnetic structure. The reduction process has, however, a more drastic effect on the anomalies: they disappear completely following the reduction process suggesting then the suppression of the Cu^{2+} 3D long-range AF order when superconductivity is induced.

II. EXPERIMENT

A superconducting $\text{Nd}_{1.85}\text{Ce}_{0.15}\text{CuO}_4$ sample ($T_c=21$ K) grown by the floating zone technique ($l_a=2.59$ mm, $l_b=1.50$ mm, $l_c=1.20$ mm) has been studied using ultrasonic interferometry in the reflection mode. In order to study the oxygenated state of $\text{Nd}_{1.85}\text{Ce}_{0.15}\text{CuO}_4$, the *same* sample has then been placed in a O_2 atmosphere at 900 °C during one week. Using a frequency feedback, the phase shift of the first reflected ultrasonic pulse is maintained constant with respect to a reference signal. Both the amplitude and the frequency variations of that pulse are measured. The use of a LiNbO_3

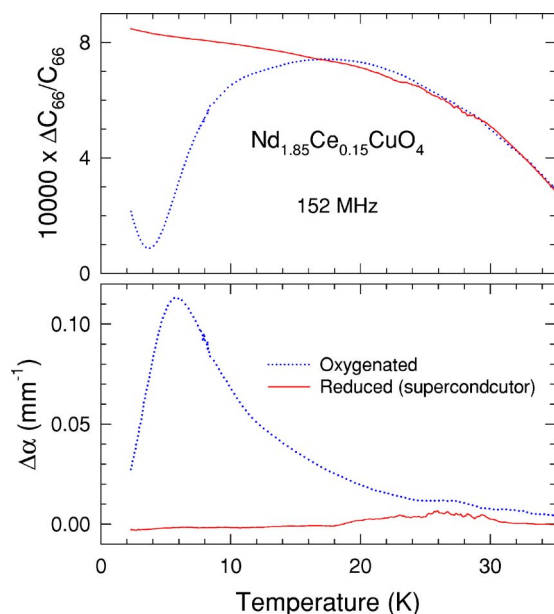


FIG. 1. (Color online) Relative variations of the elastic constant C_{66} (top panel) and corresponding variations of the sound attenuation (bottom panel) of oxygenated and reduced $\text{Nd}_{1.85}\text{Ce}_{0.15}\text{CuO}_4$ at 152 MHz.

transducer allows us to generate and detect, at 26 MHz and corresponding odd overtones, transverse waves propagating along the a axis and polarized along the b axis (C_{66}). While the absolute attenuation and elastic constant values are not accessible, the variations of the sound attenuation $\alpha(T)$ - $\alpha(40\text{ K})$ and the relative variations of the elastic constant $[C_{66}(T) - C_{66}(40\text{ K})]/C_{66}(40\text{ K})$ are obtained with high accuracy. These quantities have been obtained in the 2–40 K temperature range. In order to confirm that the ultrasonic anomalies have a magnetic origin, a magnetic field has also been applied along the a axis.

III. RESULTS AND DISCUSSION

While the spin reorientations found around 33 (Refs. 13–15) and 67 K (Ref. 15) in Nd_2CuO_4 are not detected in the doped samples, the ultrasonic anomalies below 10 K are still observed in the $\text{Nd}_{1.85}\text{Ce}_{0.15}\text{CuO}_4$ oxygenated sample. We present in Fig. 1 the temperature dependence below 35 K of the ΔC_{66} elastic moduli and the corresponding ultrasonic attenuation $\Delta\alpha$ at 152 MHz of an oxygenated $\text{Nd}_{1.85}\text{Ce}_{0.15}\text{CuO}_4$ sample (dotted curves), which show such anomalies. At this frequency, ΔC_{66} and $\Delta\alpha$ have been, respectively, reduced by a factor of 34 and 16 relative to their values in Nd_2CuO_4 .¹⁵ Even though weakened, broadened, and shifted to higher temperatures, these anomalies show temperature profiles that are similar to the ones observed in Nd_2CuO_4 : a pronounced softening of ΔC_{66} is accompanied by an attenuation peak, in agreement with a previous ultrasonic study.¹⁴ The position of the attenuation peak does not correspond to the minimum of the elastic constant, but is rather close to the maximum of the $\Delta C_{66}(T)$ temperature derivative designed as T_a , suggesting a resonant phenomenon as in Nd_2CuO_4 .¹⁵

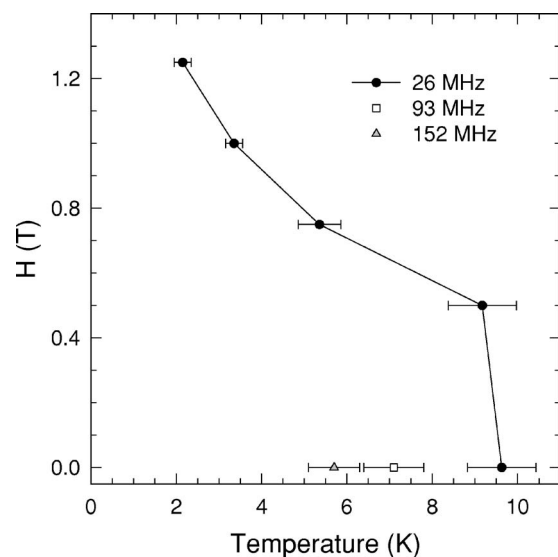


FIG. 2. Magnetic field dependence of the critical temperature T_a (see the text) observed at 26 MHz in oxygenated $\text{Nd}_{1.85}\text{Ce}_{0.15}\text{CuO}_4$, and frequency dependence of T_a in absence of magnetic field. The field is applied along the a axis (propagation direction).

The comparison with the undoped crystal is reinforced when frequency and magnetic field effects are examined. The results are summarized in Fig. 2 where the temperature T_a is mapped as a function of frequency and magnetic field. In zero field, T_a decreases with increasing frequency, going from 9.6 K at 26 MHz to 5.7 K at 152 MHz; in Nd_2CuO_4 , at approximately the same frequencies, the displacement was only from 5 to 4 K.¹⁵ When a magnetic field is applied along the a axis (Cu-O bonds), the downshift of T_a is again similar to what is observed in the undoped material. In Fig. 2, at 26 MHz, T_a decreases with a near quadratic dependence with field up to 0.7 T (2 T in Nd_2CuO_4); over this field range, frequency effects are clearly observed. At higher field values, a quasilinear decrease is rather obtained up to 1.25 T (4 T in Nd_2CuO_4) where the anomalies are no more detected in our experimental temperature range; frequency effects are absent over this range. In the oxygenated optimally doped crystal, we thus conclude that the low temperature anomalies result from the same resonant phenomenon as in the undoped one. The main differences with the pure Nd_2CuO_4 crystal are the temperature and magnetic field scales over which the phenomenon is observed and the reduced amplitude of the anomalies.

In the optimally doped $\text{Nd}_{1.85}\text{Ce}_{0.15}\text{CuO}_4$ crystal, the non-observation of the elastic anomalies due to the reorientation transitions at 33 and 67 K and the reduced amplitude of the low-temperature anomalies are clearly coherent with a reduction of the magnetic couplings as compared with the undoped compound. On the one hand, the decrease of the average magnetic moment on the Cu^{2+} sites due to the injection of mobile carriers in the CuO_2 planes should affect the Nd^{3+} - Cu^{2+} interactions. On the other hand, it is also expected that the $\text{Nd}^{3+} \rightarrow \text{Ce}^{4+}$ substitution dilutes the Nd^{3+} - Nd^{3+} interactions. Nonetheless, these interactions are not affected in the same way following Ce doping. As previously proposed,¹⁵ the low-temperature ultrasonic anomalies are re-

lated to the competition between the $\text{Nd}^{3+}\text{-Cu}^{2+}$ and the $\text{Nd}^{3+}\text{-Nd}^{3+}$ interactions, the latter one becoming important at low temperature due to the rapidly increasing moment of the Nd^{3+} Kramers ions.¹⁵ Hence, the increase in zero applied field of T_a with increasing Ce content indicates that this competition is found at higher temperature in the doped samples, suggesting that the $\text{Nd}^{3+}\text{-Cu}^{2+}$ interactions are more suppressed by Ce doping than the other ones. Moreover, this assumption is also consistent with the shift of the $H\text{-}T$ line observed in the frequency-independent regime previously associated with a noncollinear \rightarrow collinear transition of the Nd^{3+} magnetic sublattice configuration.¹⁵ Hence, this shift toward lower temperatures and lower magnetic fields, as compared to Nd_2CuO_4 , indicates that the $\text{Nd}^{3+}\text{-Nd}^{3+}$ interactions compete more efficiently with the $\text{Nd}^{3+}\text{-Cu}^{2+}$ interactions. This allows the Nd^{3+} sublattice to align in a collinear magnetic configuration at a lower field than in the undoped materials, rather than align in the noncollinear one otherwise imposed by the Cu^{2+} sublattice.

Even though weakened by Ce doping, the ultrasonic anomalies at low temperature and the magnetic interactions responsible for them remain in the oxygenated and as-grown doped samples, indicating a long-range AF ordering of the Nd^{3+} and Cu^{2+} sublattices, at least on a scale compatible with the ultrasonic characteristic length and time scales. In order to determine if the $\text{Nd}^{3+}\text{-Cu}^{2+}$ and the $\text{Nd}^{3+}\text{-Nd}^{3+}$ interactions are affected by the reduction process, we have performed ultrasonic measurements on the same $\text{Nd}_{1.85}\text{Ce}_{0.15}\text{CuO}_4$ crystal in the reduced state. The results are reported in Fig. 1 (plain curves). While the temperature profile of $\Delta C_{66}/C_{66}$ above 15 K is not significantly modified by the oxygen content, the ultrasonic anomaly observed below 10 K in the oxygenated sample is not observed in the reduced one. Similarly, the corresponding peak of attenuation observed for the oxygenated sample disappears after the reduction process. These observations indicate a strong modification of the magnetic ordering, and raises the question: how the reduction process can affect the magnetic properties of the optimally doped samples? Since the amount of oxygen removed in this process is very tiny, the crystal-field parameters deduced from the Nd^{3+} ions within the bulk $\text{Nd}_{2-x}\text{Ce}_x\text{CuO}_4$ structure are not affected,¹² suggesting that the probed structure is not significantly changed. This is consistent with the invariance of the $\Delta C_{66}/C_{66}$ temperature profile above 15 K. At least, this indicates that the elastic constant is not affected by the presence of the $(\text{Nd,Ce})_2\text{O}_3$ epitaxial impurity phase observed by neutron scattering,^{16–18} which occupies a volume much smaller than 1% in optimally doped samples. For these reasons, we do not expect any direct effect on the Nd^{3+} magnetic moment as well as on the $\text{Nd}^{3+}\text{-Nd}^{3+}$ interactions.

In Nd_2CuO_4 , the resonant phenomenon responsible for the low-temperature ultrasonic anomalies is quite well described by a resonant frequency $\nu_0(T)$ and a damping coefficient $\Gamma(T)$ which vary rapidly in temperature proportionally to the Nd^{3+} paramagnetic susceptibility $\chi(\mathbf{q}=0, T)$ and its inverse, respectively.¹⁵ While the magnetic susceptibility is related to the $\text{Nd}^{3+}\text{-Nd}^{3+}$ interactions, the effect of the $\text{Nd}^{3+}\text{-Cu}^{2+}$ is somehow included in the proportionality coefficients. As shown experimentally^{19,20} and expected theoretically owing to its nearly unperturbed structure, the overall

$\text{Nd}_{2-x}\text{Ce}_x\text{CuO}_4$ magnetic susceptibility, which is mainly governed by the Nd^{3+} paramagnetic susceptibility, is not significantly affected by the reduction process. Hence, only the proportionality coefficients in the resonant model are allowed to vary. Furthermore, no direct ordering of the Nd^{3+} subsystem following the reduction, that could modify the magnetic susceptibility, is observed above 2 K. The fact that the Nd^{3+} sublattice is not directly affected by the reduction is also supported by the comparison with other rare earth compounds.

Similar to $\text{Nd}_{2-x}\text{Ce}_x\text{CuO}_4$, the $\text{Sm}^{3+}\text{-Sm}^{3+}$ interactions and the ordering of the Sm^{3+} sublattice in $\text{Sm}_{2-x}\text{Ce}_x\text{CuO}_4$ are not affected by the reduction process, as shown by ultrasonic and specific heat measurements.²¹ In contrast to the Sm^{3+} moments in $\text{Sm}_{2-x}\text{Ce}_x\text{CuO}_4$, the Nd^{3+} moments in $\text{Nd}_{2-x}\text{Ce}_x\text{CuO}_4$ are strongly coupled with the Cu^{2+} sublattice and can be used to probe the magnetic properties of the CuO_2 planes. It follows from the comparison between $\text{Nd}_{2-x}\text{Ce}_x\text{CuO}_4$ and $\text{Sm}_{2-x}\text{Ce}_x\text{CuO}_4$ that if the reduction process affects strongly the low-temperature ultrasonic anomalies in $\text{Nd}_{2-x}\text{Ce}_x\text{CuO}_4$, which originate from the competition between the $\text{Nd}^{3+}\text{-Cu}^{2+}$ and the $\text{Nd}^{3+}\text{-Nd}^{3+}$ interactions, it is necessarily due to $\text{Nd}^{3+}\text{-Cu}^{2+}$ interactions via the Cu^{2+} sublattice. The corollary to the previous remarks is the suppression of the Cu^{2+} long-range 3D AF order.

The explanation for such variations in the magnetic properties, which support a competition between AF and superconductivity, must be found in the small structural modifications induced by the reduction process necessary to achieve superconductivity. Until recently, it has been generally accepted that the oxygens removed in the reduction process are located in interstitial sites, above copper ions [apical oxygen O(3)]. Contrary to this widespread belief, Raman and crystal-field infrared transmission studies on $\text{Pr}_{2-x}\text{Ce}_x\text{CuO}_4$ (Ref. 11) and $\text{Nd}_{2-x}\text{Ce}_x\text{CuO}_4$,^{12,22} as a function of the oxygen content, have shown that while the amount of apical oxygens increases with doping, these oxygens are not removed by the reduction of doped samples. It was also shown that the type of oxygen removed in the reduction process depends on the cerium concentration. The authors proposed that oxygens are removed mostly from the charge reservoirs [O(2)] at low doping, while only oxygens in the CuO_2 planes [O(1)] are removed at high doping ($x \geq 0.1$).^{11,12} Actually, such in-plane oxygen vacancies created after the reduction process would be likely candidates to destroy the Cu^{2+} long-range AF order, thus affecting the ultrasound anomalies.

In a competing scenario, the $(\text{Nd,Ce})_2\text{O}_3$ epitaxial impurity phase, observed recently by neutron scattering and confirmed by high-resolution TEM,^{16–18} is created in order to remove Cu^{2+} vacancies in the CuO_2 planes, making the remaining structure more perfect for superconductivity.²³ Unfortunately, the correction of the Cu nonstoichiometry in the CuO_2 planes after the sample reduction has not been directly confirmed yet by any local probe. Furthermore, the authors of this scenario suggested an increase of carriers introduced by the oxygen reduction, in contrast to a recent Hall effect study, which has shown that the carrier mobilities rather than their concentrations are significantly changed by the reduction process, preventing us to attribute these magnetic modifications to a simple dilution of the Cu^{2+} sublattice due to a

simple addition of carriers.²⁴ While one cannot conclude at this stage on a particular scenario of the microscopic details of the reduction process, it is clear from our ultrasonic results that superconductivity emerges from the competing AF order, probably by modifying the local structure rather than by introducing carriers. The suppression of the long-range AF 3D order, which acts as a source of localization, is believed to largely enhance the transport properties in the reduced materials. As for the short-range AF order, its persistence in the superconducting state is supported by Hubbard model calculations,^{25,26} which indicate that short-range AF fluctuations are responsible for the loss of spectral weight observed in the ARPES spectra of superconducting $\text{Nd}_{2-x}\text{Ce}_x\text{CuO}_4$ samples at the crossing of the Fermi surface and the first magnetic Brillouin zone.^{27,28} Unfortunately, the detail of the interplay between the short-range AF order and the superconducting state is not completely clarified yet and would need to be studied more thoroughly using local probes.

IV. CONCLUSION

In summary, we have first discussed the influence of the cerium content on the $\text{Nd}^{3+}\text{-Cu}^{2+}$ and the $\text{Nd}^{3+}\text{-Nd}^{3+}$ interac-

tions. As illustrated by the temperature dependence of low-temperature frequency-dependent ultrasonic anomalies, we have shown that the latter is less influenced than the former one by Ce doping. Nevertheless, the ultrasonic anomalies persist in the oxygenated optimally doped samples, and they are suppressed only after the reduction process. While the detail of the reduction process remains an open issue, this indicates that the Cu^{2+} long-range 3D AF order is destroyed by the reduction process, thus favoring the emergence of superconductivity in these materials.

ACKNOWLEDGMENTS

We thank M. Castonguay for technical assistance, as well as A. A. Nugroho and A. A. Menovsky who provided us samples. We also acknowledge support from the National Sciences and Engineering Research Council of Canada (NSERC) and le Fonds Québécois de la Recherche sur la Nature et les Technologies (FQRNT) du Gouvernement du Québec.

*Electronic address: richarpi@bc.edu

- ¹H. J. Kang, P. Dai, J. W. Lynn, M. Matsuura, J. R. Thompson, S.-C. Zhang, D. N. Argyriou, Y. Onose, and Y. Tokura, *Nature* (London) **423**, 522 (2003).
- ²K. Yamada, K. Kurahashi, T. Uefuji, M. Fujita, S. Park, S.-H. Lee, and Y. Endoh, *Phys. Rev. Lett.* **90**, 137004 (2003).
- ³E. Moran, A. I. Nazzari, T. C. Huang, and J. B. Torrance, *Physica C* **160**, 30 (1989).
- ⁴J. S. Kim and D. R. Gaskell, *Physica C* **209**, 381 (1993).
- ⁵E. Wang, J.-M. Tarascon, L. H. Greene, G. W. Hull, and W. R. McKinnon, *Phys. Rev. B* **41**, 6582 (1990).
- ⁶E. Takayama-Muromachi, F. Izumi, Y. Uchida, K. Kato, and H. Asano, *Physica C* **159**, 634 (1989).
- ⁷K. Susuki, K. Kishio, T. Hasegawa, and K. Kitazawa, *Physica C* **166**, 357 (1990).
- ⁸M. Matsuda, Y. Endoh, K. Yamada, H. Kojima, I. Tanaka, R. J. Birgeneau, M. A. Kastner, and G. Shirane, *Phys. Rev. B* **45**, 12548 (1992).
- ⁹T. Uefuji, K. Kurahashi, M. Fujita, M. Matsuda, and K. Yamada, *Physica C* **378-381**, 273 (2002).
- ¹⁰P. K. Mang, O. P. Vajk, A. Arvanitaki, J. W. Lynn, and M. Greven, *Phys. Rev. Lett.* **93**, 027002 (2004).
- ¹¹G. Riou, P. Richard, S. Jandl, M. Poirier, P. Fournier, V. Nekvasil, S. N. Barilo, and L. A. Kurnevich, *Phys. Rev. B* **69**, 024511 (2004).
- ¹²P. Richard, G. Riou, I. Hetel, S. Jandl, M. Poirier, and P. Fournier, *Phys. Rev. B* **70**, 064513 (2004).
- ¹³V. D. Fil', G. A. Zvyagina, S. V. Zherlitsyn, I. M. Vitebsky, V. L. Sobolev, S. N. Barilo, and D. I. Zhigunov, *Mod. Phys. Lett. B* **5**, 1367 (1991).
- ¹⁴S. V. Zherlitsyn, G. A. Zvyagina, V. D. Fil', I. M. Vitebskii, S. N. Barilo, and D. I. Zhigunov, *Low Temp. Phys.* **19**, 934 (1993).
- ¹⁵P. Richard, M. Poirier, and S. Jandl, *Phys. Rev. B* **71**, 144425

- (2005).
- ¹⁶K. Kurahashi, H. Mastushita, M. Fujita, and K. Yamada, *J. Phys. Soc. Jpn.* **71**, 910 (2002).
- ¹⁷M. Matsuura, P. Dai, H. J. Kang, J. W. Lynn, D. N. Argyriou, K. Prokes, Y. Onose, and Y. Tokura, *Phys. Rev. B* **68**, 144503 (2003).
- ¹⁸P. K. Mang, S. Larochelle, A. Mehta, O. P. Vajk, A. S. Erickson, L. Lu, W. J. L. Buyers, A. F. Marshall, K. Prokes, and M. Greven, *Phys. Rev. B* **70**, 094507 (2004).
- ¹⁹C. Mennerich, D. Baabe, D. Mienert, F. J. Litterst, P. Adelman, and H.-H. Klauss, *J. Magn. Magn. Mater.* **272-276**, 162 (2004).
- ²⁰N. Ravindran, T. Sarkar, S. Uma, G. Rangarajan, and V. Sankaranarayanan, *Phys. Rev. B* **52**, 7656 (1995).
- ²¹I. Hetel, Master thesis, Université de Sherbrooke, Sherbrooke, Canada, 2002.
- ²²P. Richard, G. Riou, S. Jandl, M. Poirier, P. Fournier, V. Nekvasil, and M. Diviš, *Physica C* **408-410**, 830 (2004).
- ²³H. J. Kang, P. Dai, H. A. Mook, D. N. Argyriou, V. Sil'chenko, J. W. Lynn, Y. Kurita, S. Komiya, and Y. Ando, *Phys. Rev. B* **71**, 214512 (2005).
- ²⁴J. Gauthier, S. Gagné, J. Renaud, M.-E. Gosselin, P. Richard, and P. Fournier (to be published).
- ²⁵D. Sénéchal and A.-M. S. Tremblay, *Phys. Rev. Lett.* **92**, 126401 (2004).
- ²⁶B. Kyung, V. Hankevych, A.-M. Daré, and A.-M. S. Tremblay, *Phys. Rev. Lett.* **93**, 147004 (2004).
- ²⁷N. P. Armitage, F. Ronning, D. H. Lu, C. Kim, A. Damascelli, K. M. Shen, D. L. Feng, H. Eisaki, Z.-X. Shen, P. K. Mang, N. Kaneko, M. Greven, Y. Onose, Y. Taguchi, and Y. Tokura, *Phys. Rev. Lett.* **88**, 257001 (2002).
- ²⁸H. Matsui, K. Terashima, T. Sato, T. Takahashi, S.-C. Wang, H.-B. Yang, H. Ding, T. Uefuji, and K. Yamada, *Phys. Rev. Lett.* **94**, 047005 (2005).